Silicon Nanowires Loaded with Iron Phosphide for Effective Solar-Driven Hydrogen Production

Cuncai Lv,[a] Zhibo Chen,[a] Zhongzhong Chen,[a] Bin Zhang,[b] Yong Qin,[b] Zhipeng Huang,*[a] and Chi Zhang*[a]

a. Functional Molecular Materials Research Centre, Scientific Research Academy, Jiangsu University, Zhenjiang 212013, P. R. China. Email: zphuang@ujs.edu.cn; chizhang@ujs.edu.cn.

b. State Key Laboratory of Coal Conversion, Institute of Coal Chemistry, Chinese Academy of Science, Taiyuan 030001, P.R. China.

Supporting Information

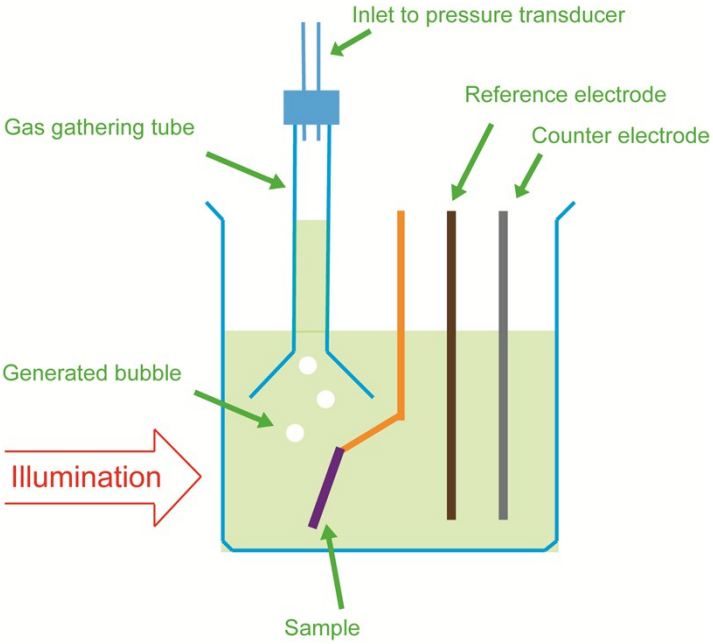

Figure S1. Illustration of the setup used to monitor the volume of generated gas.

If the initial height of water in the gas gathering tube before the gas gathering experiment is h_0, and after the *i-t* experiment the generated gas is gathered into the tube and the final height of water in the gas gathering tube become h_1, then the volume of generated gas (V) should be $s(h_0-h_1)$, where s is the inner cross-sectional area of the gas gathering tube.

At the initial status, the pressure inside the gas gathering tube (P_0) is $P - \rho g h_0$, where P is the atmospheric pressure, ρ is the density of water, and g is the acceleration due to gravity. The output voltage of the differential pressure transducer would be $U_0 = k(P - P_0) = k\rho g h_0$, where k is the sensitivity of the differential pressure transducer (1 mV/Pa for a Freescale MPXV7002DP). When the height of water in the gas gathering tube decreases to h_1, the pressure inside the gas gathering tube becomes P_1, and $P_1 = P - \rho g h_1$. Then, the output of the differential pressure transducer is $U_1 = k(P - P_1) = k\rho g h_1$.

Accordingly, the volume of generated gas can be computed by $V = s(h_0 - h_1) = s(U_0/k\rho g - U_1/k\rho g) = s(U_0 - U_1)/k\rho g = C(U_0 - U_1)$, where C is a coefficient that can be calibrated by injecting a known volume of gas into the gas gathering tube and recording the variation of output voltage of the differential pressure transducer.

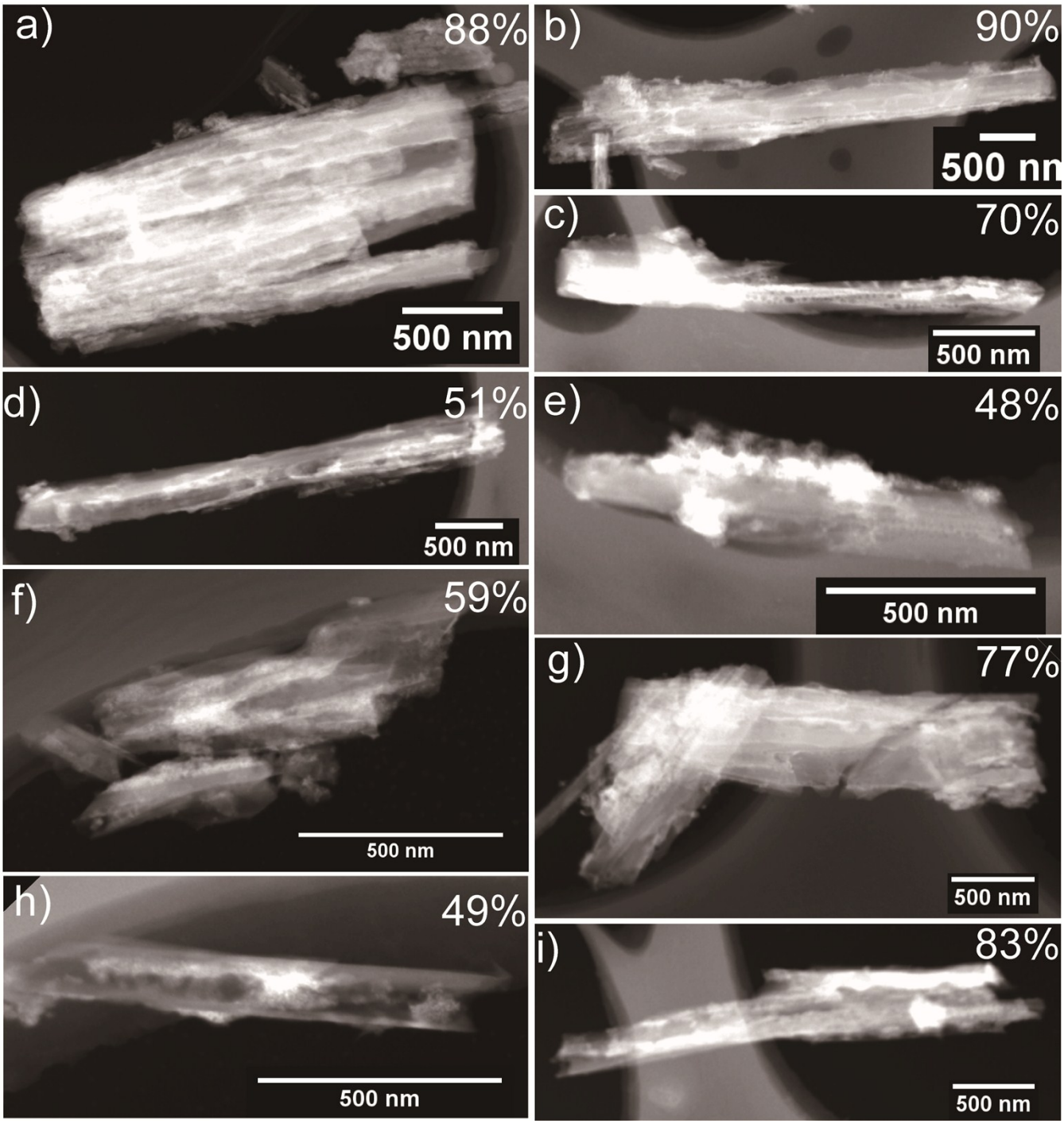

Figure S2. STEM image of the SiNWs/FeP. The value on the upper right corner of each image is the coverage of FeP on the surface of SiNWs estimate by software ImageJ. The coverage is computed by the projected area of FeP (component with brighter contrast in STEM image) divided by the projected area of SiNW.

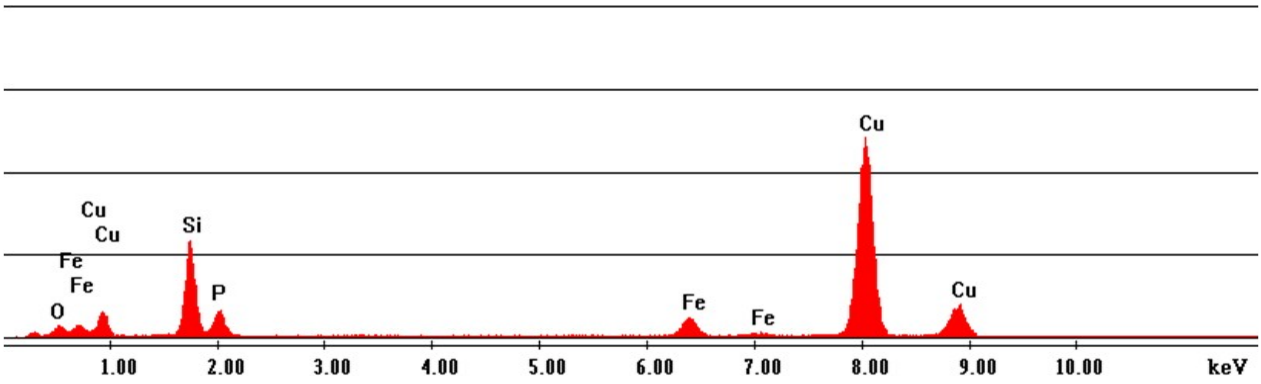

Figure S3. EDX spectrum of SiNWs/FeP recorded in TEM. The signal of Cu comes from the copper grid used to support the SiNWs/FeP.

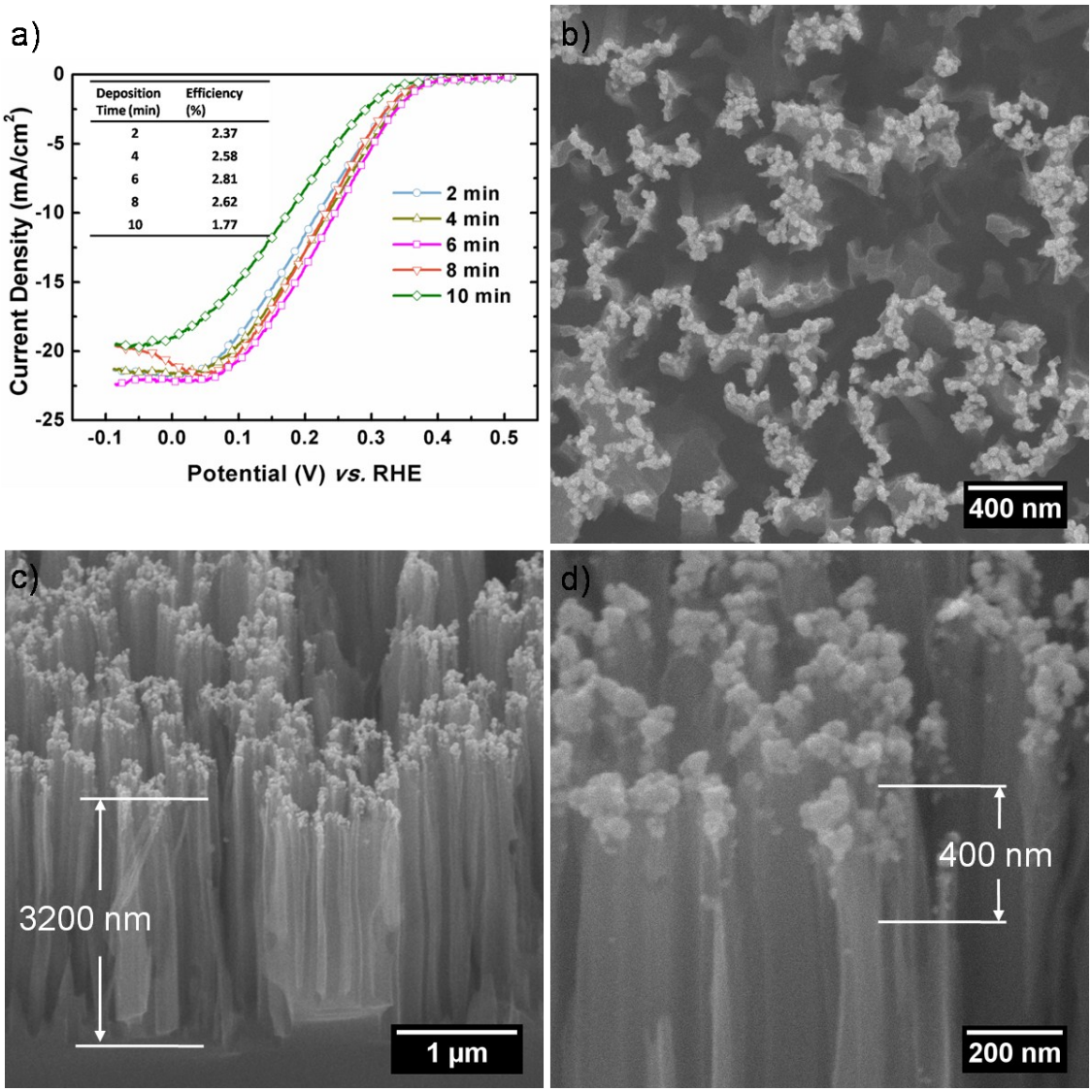

Figure S4. (a) Polarization curves of SiNWs subjected to Pt electroless deposition with different times. Inset shows the efficiency corresponding to different deposition times of Pt. (b) Plan-view and (c,d) bird-eye's view SEM image of SiNWs/PtNPs with the optimal performance, which was subjected to 6 min Pt electroless deposition. In bird-eye's view SEM image the sample was 45° tilted.

The optimal PCE of SiNWs/PtNPs sample is 2.81% in our experiment (Illumination intensity: 100 $mW \cdot cm^2$). In order to introduce Pt nanoparticles to SiNWs, SiNWs sample was first immersed diluted HF for 5 min to remove surface oxide, and Pt nanoparticles are deposited by immersion of SiNWs into a solution of 0.4 M HF and 1mM K_2PtCl_6 for different times. Afterwards, the SiNWs samples loaded with Pt nanoparticles were rinsed with copious amount of deionized water and dried in air.

In SiNWs/PtNPs sample, nearly very SiNW was loaded with PtNPs (Figure S4b). For SiNWs with typical length of 3200 nm, PtNPs were found only on the top region of SiNWs, and the length of this region was smaller than 400 nm (Figure S4c and Figure S4d). It is therefore reasonable to estimate that the coverage of Pt on SiNWs was less than 12.5%.

Table S1. Key performance of reported results and the corresponding measurement conditions.

Ref	photocathode	catalyst	J_{sc} (mA/cm^2)	V_{oc} (V)	PCE (%)	Illumination intensity (mW/cm^2)	Light source
[1]	planar Si, p-n^+ junction	Pt	18.80	0.49	5.5	38.6	simulated AM 1.5 spectrum, λ>635 nm
	planar Si, p-n^+ junction/Ti		17.85	0.51	6.16		
	planar Si, p-n^+ junction/Ti/TiO_2		21.68	0.51	7.77		
[2]	planar Si, p-n^+ junction/Ti	MoS_x	16.4	0.368	7.46	38.6	simulated AM 1.5 spectrum, λ>635 nm
		Pt	14.87	0.48	11.66		
[3]	Si microwires, core-shell p-n^+ junction	Ni-Mo	9.1	0.46	2.21	100	ELH-type W-halogen lamp, AM 1.5G filter
[4]	Si microwires, core-shell p-n^+ junction	Pt	15	0.54	5.8	100	ELH-type W-halogen lamp
	Si microwires		7.3	0.16	0.21		
	planar Si, p-n^+ junction		28	0.56	9.6		
	planar Si		23	0.30	2.1		
[5]	Si nanowires	$Ni_{12}P_5$	21.0	0.40	2.97	100	Xe lamp
[6]	Si nanowires	MoS_3	24.9	0.36	2.28	100	ELH-type W-halogen lamp
[7]	Si nanowires	WS_3	19.0	0.40	2.02	100	Xe lamp
[8]	planar Si/Au film	Pt	16.7	0.274	0.753	100	halogen lamp
	planar Si		16.9	0.265	0.784		
[9]	Si nanowires	Pt	17	0.42	2.73	100	halogen lamp
	planar Si		27	0.33	2.13		
[10]	Si nanowires	MoS_2	1	0.25	0.03	100	Xe lamp with 400 nm cut-off filter
[11]	Si micro-pillar	Mo_3S_4 cluster	9.45	0.14	1.236	28.3	Xe-arc lamp simulated AM1.5G radiation, λ>635 nm
[12]	Nanoporous black Si	___	2.3	0.1	0.024	100	simulated AM1.5 illumination
[13]	Tapered Si nanohole arrays	___	7.5	0.15	0.13	100	under AM 1.5 G illumination
[14]	Nanoporous Si	___	30.6	0.26	2.63	100	Xe lamp with an AM1.5 filter
		Pt	28.4	0.4	3.23		
[15]	20μm-thin Si nanoholes	Pt	23.1	0.31	1.19	100	a solar simulator (Peccel PEC-L11) under AM 1.5G illumination
[16]	350μm thick p^+pn^+-Si(front)		24.6	0.52	19.18		

	50μm thick p^+pn^+-Si(front)	Pt	23.6	0.52	19.1	41.8	Xenon lamp with a 635 nm cut-off filter and an AM1.5 filter,λ>635 nm
	30μm thick p^+pn^+-Si(front)		20.3	0.5	15.7		
	350μm thick p^+pn^+-Si(back)		6.4	0.49	5.4		
	50μm thick p^+pn^+-Si(back)		16.8	0.5	13.2		
	30μm thick p^+pn^+-Si(back)		16.0	0.5	12.4		
[17]	Amorphous Si thin film	Pt	11.6	0.93	5.87	100	a solar simulator (Solar Light, model 16S-300-005) with AM 1.5 filter

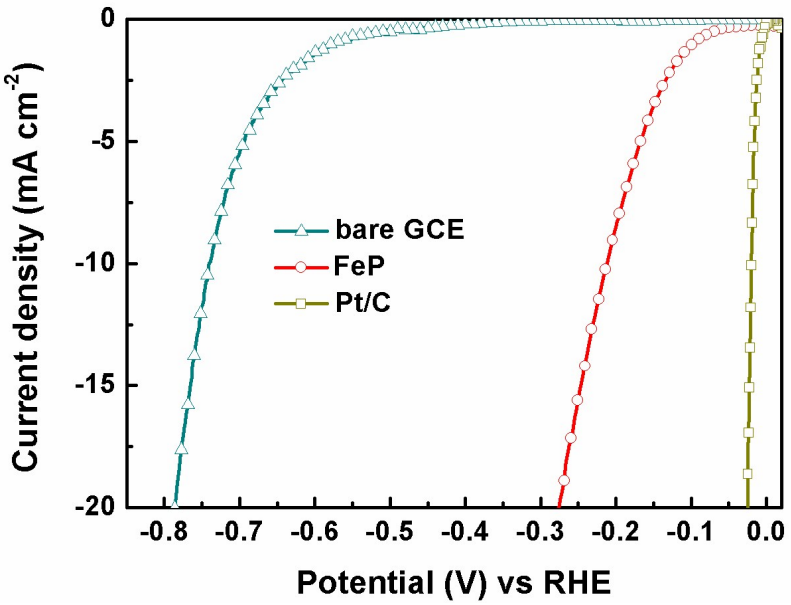

Figure S5. The polarization curves of FeP, commercial Pt/C (Johnson Matthey, Hispec 3000, 20 wt.%), and a bare glassy carbon electrode (GCE) in 0.5 M H_2SO_4 solution. The loading of FeP and Pt/C is 0.285 mg cm^{-2}. All potentials are corrected with iR drop.

All measurements were carried out in a three-electrode electrochemical cell. The FeP or Pt/C were loaded onto GCE (3 mm diameter) which was used as a working electrode; a graphite rod (6 mm diameter) was employed as a counter electrode, and a mercury/mercurous sulfate electrode (MSE) was used as a reference electrode. The counter electrode was separated from the working chamber by a porous glass frit. To load catalyst onto the GCE, a dispersion of the catalyst (4 mg) and Nafion solution (5 wt. %, 80 μL) in 1 ml of water/ethanol (4/1, v/v) was ultrasonicated using an ultrasonic probe (2 mm diameter, 130 W) for 1 h to form a homogeneous ink, and then 5 μL of the ink was dropped onto the polished GCE. The RHE was determined to be -0.694 V *versus* MSE for the 0.5 M H_2SO_4 solution by the open circuit potential of a clean Pt electrode in the solution of interest purged with H_2 (99.999%). Polarization curves were measured at a sweep rate of 5 mV s^{-1}. The current-interrupt method was employed to measure the uncompensated cell resistance (R).

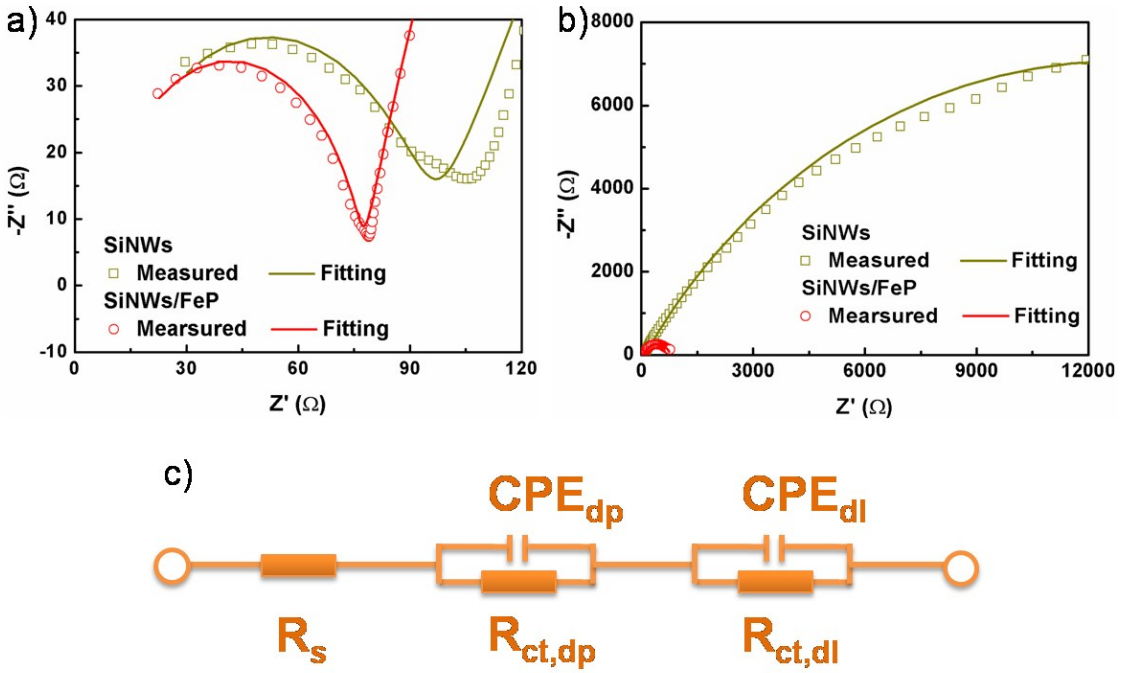

Figure S6. (a,b) EIS spectra of the SiNWs and the SiNWs/FeP, (c) A equivalent circuit used for the data fitting of EIS spectra. R_s represents the overall series resistance of the circuit, CPE_{dp} is the capacitance phase element for the depletion layer of semiconductor, $R_{ct,dp}$ is the charge transfer resistance in the depletion layer of semiconductor, CPE_{dl} is the capacitance phase element for double layer at semiconductor/electrolyte interface, and $R_{ct,dl}$ is the charge transfer resistance of double layer at semiconductor/electrolyte interface.

Table S2. Values of elements in the equivalent circuit (Figure S5) resulted from fitting the EIS data.

Sample	R_s (Ω)	Q_{dl} ($F\ cm^{-2}\ S^{n-1}$)	n_{dl}	$R_{ct,dl}$ (Ω)	Q_{dp} ($F\ cm^{-2}\ S^{n-1}$)	n_{dp}	$R_{ct,dp}$ (Ω)
SiNWs	6.004	4.26e-5	0.6435	25540	2.732e-8	0.8759	87.25
error (%)	138.5	3.343	1.048	3.55	93.23	8.542	11.02
SiNWs/FeP	5.915	1.153e-5	0.8226	689.1	9.289e-9	0.9611	70.78
error (%)	29.69	4.713	0.7848	1.176	26.55	2.159	2.91

Reference

1. B. Seger, T. Pedersen, A. B. Laursen, P. C. K. Vesborg, O. Hansen and I. Chorkendorf, *J. Am. Chem. Soc*, 2013, **135**, 1057-1064.
2. B. Seger, A. B. Laursen, P. C. K. Vesborg, T. Pedersen, O. Hansen, S. Dahl and I. Chorkendorff, *Angew. Chem. Int. Ed.*, 2012, **51**, 1-5.
3. E. L. Warren, J. R. McKone, H. A. Atwater, H. B. Gray and N. S. Lewis, *Energy Environ. Sci.*, 2012, **5**, 9653-9661.
4. S. W. Boettcher, E. L. Warren, M. C. Putnam, E. A. Santori, D. Turner-Evans, M. D. Kelzenberg, M. G. Walter, J. R. McKone, B. S. Brunschwig, H. A. Atwater and N. S. Lewis, *J. Am. Chem. Soc.*, 2011, **133**, 1216-1219.
5. Z. Huang, Z. Chen, Z. Chen, C. Lv, H. Meng and C. Zhang, *ACS Nano*, 2014, **8**, 8121-8129.
6. Z. Huang, C. Wang, L. Pan, F. Tian, X. Zhang and C. Zhang, *Nano Energy*, 2013, **2**, 1337-1346.
7. Z. P. Huang, C. F. Wang, Z. B. Chen, H. Meng, C. C. Lv, Z. Z. Chen, R. Q. Han and C. Zhang, *Acs Applied Materials & Interfaces*, 2014, **6**, 10408-10414.
8. J. Kye, M. Shin, B. Lim, J.-W. Jang, I. Oh and S. Hwang, *ACS Nano*, 2013, **7**, 6017-6023.
9. I. Oh, J. Kye and S. Hwang, *Nano Lett*, 2013, **12**, 298-302.
10. P. D. Tran, S. S. Pramana, V. S. Kale, M. Nguyen, S. Y. Chiam, S. K. Batabyal, L. H. Wong, J. Barber and J. Loo, *Chemistry-a European Journal*, 2012, **18**, 13994-13999.
11. Y. Hou, B. L. Abrams, P. C. K. Vesborg, M. E. Björketun, K. Herbst, L. Bech, A. M. Setti, C. D. Damsgaard, T. Pedersen, O. Hansen, J. Rossmeisl, S. Dahl, J. K. Nørskov and I. Chorkendorff, *Nature materials*, 2011, **10**, 434-438.
12. J. Oh, T. G. Deutsch, H.-C. Yuan and H. M. Branz, *Energy Environ. Sci.*, 2011, **4**, 1690-1694.
13. J.-Y. Jung, M. J. Choi, K. Zhou, X. Li, S.-W. Jee, H.-D. Um, M.-J. Park, K.-T. Park, J. H. Bang and J.-H. Lee, *J. Mater. Chem. A.*, 2014, **2**, 833-842.
14. Y. Zhao, N. C. Anderson, K. Zhu, J. A. Aguiar, J. A. Seabold, J. v. d. Lagemaat, H. M. Branz and N. R. Neale, *Nano Lett.*, 2015, **15**, 2517-2525.
15. J.-Y. Jung, M.-J. Park, X. Li, J.-H. Kim, R. B. Wehrspohn and J.-H. Lee, *J. Mater. Chem. A.*, 2015, **3**, 9456-9460.
16. D. Bae, T. Pedersen, B. Seger, M. Malizia, A. Kuznetsov, O. Hansen, I. Chorkendorff and P. C. K. Vesborg, *Energy Environ. Sci.*, 2014, **00**, 1-3.
17. Y. Lin, C. Battaglia, M. Boccard, M. Hettick, Z. Yu, C. Ballif, J. W. Ager and A. Javey, *Nano Lett.*, 2013, **13**, 5615-5618.